SEISMIC RESPONSE CHARACTERISTICS OF FULL-SIZE BUILDINGS WITH BASE ISOLATION SYSTEM

by

C. Y. Wang and J. Gvildys

Reactor Engineering Division
Argonne National Laboratory
Argonne, Illinois 60439, U.S.A.

ANL/CP--72574

DE91 011833

ABSTRACT

This paper investigates the response characteristics of full-size reinforced concrete buildings via numerical simulations and actual observations. The test facility consists of two identical three-story buildings constructed side by side at Tohoku University in Sendai, Japan. Since the installation of high-damping isolation bearings in April 1989, data from over twenty earthquakes have been recorded. In this paper, three representative earthquake records, #2, #6, and #17 are used to study the detailed response characteristics. Numerical simulations are carried out with the system response program, SISEC.

In general, good agreement has been found between numerical solutions and actual observations. Both results indicate that the advantage of the isolation system for small earthquakes is insignificant. For relatively large earthquake motion, however, such as from record #6 earthquake, the effect of isolators in mitigating the acceleration response becomes more pronounced. Also, both analysis and observation have demonstrated that the isolation system installed in the Sendai Building is very effective. The system is stiff enough to prevent the building displacement under minor earthquakes and wind loads, but is relatively soft for reducing the acceleration response during earthquakes with moderate and strong ground motion.

MASTER

I. INTRODUCTION

Seismic isolation is gaining attention worldwide for use in a wide spectrum of structures and critical facilities, including bridges, office buildings, hospitals, computing and telecommunication centers, as well as nuclear facilities [1-3]. Today there are over 125 structures worldwide which are isolated and the numbers have been increasing steadily in the past few years. Also, substantial research efforts have been devoted to the designs, testing of isolation bearings, as well as development of analytical methods for predicting the responses of isolated structures.

Sponsored by the National Science Foundation (NSF), Argonne National Laboratory of the USA and Shimizu Corporation of Japan initiated a joint research program in 1989 on the seismic base isolation. The aim of this program is to design, test, and analyze isolation systems in a full-size building and to obtain data on relative responses between isolated and nonisolated structures under actual earthquake conditions. This latter task of the program results from the unique design of the test facility, located at Tohoku University in Sendai, Japan (about 200 miles north of Tokyo). The test facility consists of two identical full-size three-story buildings built side by side, except that one structure is seismically isolated and the other is not. The facility can easily adapt to a variety of seismic isolated systems [4-6]. Since Sendai is quite active seismically, considerable data can be obtained in a relatively short period of time.

The isolated system installed at Sendai has been tested extensively in the laboratory. The isolation bearings are made of high-damping rubber laminated with steel plates. This type of elastomeric bearing is very attractive, particularly when adapting it to the building and nuclear

plant designs, since it combines the restoring and dissipating functions of isolator into one compact and maintenance-free unit.

Following the installation of high-damping elastomer bearings, twenty (20) earthquakes have been observed between April and December 1989 at the test facility [4]. Because the entire acceleration records are quite extensive, only data of three representative earthquakes, i.e., #2, #6, and #17 are used here to study the building response characteristics. Record #2 represents an earthquake occurring almost immediately after the bearing installation; #6 earthquake had the largest magnitude, whereas #17 had the longest duration. Numerical simulations are carried with the three-dimensional system response program SISEC developed at Argonne National Laboratory [7].

We will proceed to discuss the test facility, isolation bearing, results of observed and simulated building response characteristics.

II.   DESCRIPTION OF THE SENDAI BUILDINGS AND EARTHQUAKE OBSERVATION
       DATA

Two test buildings, one conventionally designed and other base-isolated, were constructed side by side at Tohoku University located in Sendai, in the northern part of Japan. The test buildings consist of two full-size, three-story reinforced concrete structures. The dimensions and construction details of the superstructure were exactly the same for both buildings. The buildings were constructed as rigid frame structures with outer walls made of light weight concrete panel. The plan dimensions of the building are 6 by 10 meters (19.685 by 32.808 ft). The total

combined floor areas is 180 m² (1937.49 ft²). The test buildings were completed in May 1986 [4-6].

Figure 1 shows a general view of the test buildings. The building on the left is the ordinary one, whereas on the right is the base-isolated structure. The plan and elevation of the test structures given in Fig. 2 show six isolator bearings installed in the base-isolated building. Note from this figure that the ordinary building is surrounded by a 6.56 ft (2.0 m) backfilled soil below the ground level and that the basement wall is made of reinforced concrete. The presence of soil embedment and concrete wall definitely will have certain mitigating effects on the building response. As for the isolated building, ample space is provided around the side of the basement wall to allow unrestricted movement of the superstructure. The base-isolation system consists of by six laminated steel-rubber bearings. The test buildings were built in a relatively hard loam layer containing gravel, whose shear wave velocity is 310 m/sec (1017 ft/sec).

The isolation system of the base isolated building consists of six identical bearings which were designed by ANL and manufactured in the U.S. This work was funded by the National Science Foundation under a joint research project between ANL and Shimizu Corporation. The bearings were installed by Shimizu of Japan in April 1989. These bearings are laminated composites with 33 alternating layers of high-damping rubber and steel plates (shims) manufactured by Fluorocarbon Inc., USA.[*] High-damping rubber bearing is used since it seems to be well suited for applications in seismic isolation and is currently being used or proposed to be used in many structures, including buildings and nuclear facilities.

---

[*]Now known as FURON, Structural Bearings Division.

4

Figure 3 shows the engineering details of the elastomer bearing. The outer diameter and overall height of the bearing are 508 and 284.2 mm (20 and 11 3/16 in), respectively. The design isolation frequency of the bearings, corresponding to the 50% shear strain, is 0.75 Hz. The design value for the horizontal stiffness of each bearing is 5382 lb/in, or 32.3 Kip/in for the entire isolation system (6 bearings).

The dowel joint used at the top and bottom plates of the bearing transfers lateral loads from the structure to the bearing and to the foundation. The dowels are free to move vertically. The response characteristics of the laminated bearings were determined by the Shimizu Institute of Technology through the conduct os series of static and dynamic tests on two bearings (identical to those installed in the building). Detailed test results, labelled as test specimens Nos. 1 and 2, are given in Ref. [4].

To illustrate the test data, Fig. 4 presents the equivalent stiffness and damping ratio as a function of relative horizontal displacement between the top and bottom of the isolator bearing. The data were taken from test specimen Nos. 1 and 2, the static loading experiment of Tohoku University test building, as well as data generated when Bridgestone Rubber Company bearings had been installed in the test building before the ANL tests. It is worthwhile to note that the stiffness and damping ratio obtained from the site experiment are somewhat lower than those obtained from individual bearing tests. Figure 4a indicates that as the horizontal displacement increases, the bearing horizontal stiffness decreases. Thus, small displacement caused by minor earthquakes the isolator horizontal stiffness would be very high (much higher than the designed value of 0.75 Hz). Figure 4b indicates that for very small displacements (about 0.4 cm), the damping ratio obtained by the site experiment is about 10%. As the displacement amplitude

increases, the damping ratio will first increase and then decrease to 8% at displacement of 8.5 cm. Damping ratios for displacements less than 0.4 cm are not available from either the specimen test or site experiment.

Since the installation of ANL-designed isolation bearings on April 17, 1989, 20 earthquakes have been observed at the test facility. Records of these events have been transmitted to ANL. Since the entire acceleration records are quite extensive, only one representative earthquake record, i.e., record #6, is used for the discussion of code validation for the SISEC code in this preliminary report. Reference [4] contains information regarding the magnitudes, distributions of epicenters, and epicentral distance of all of these earthquakes. From the records it appears that earthquake #6 has the strongest ground motion at the test site.

III.   MATHEMATICAL MODEL AND BUILDING FREQUENCY

Three-dimensional frame models are used in the SISEC code simulations for both convention and base-isolated buildings. In the analyses, beams, columns, and girders are all modeled by 3-D beam elements with six degrees of freedom per note to account for the translations and rotations generated from seismic events. Stiffnesses of the outer walls and partitions that are not structurally connected to the beams and girders are neglected in the calculation. However, their masses are appropriately lumped to the element nodal points, so that their inertia effects are included in the analysis.

The mathematical models of both ordinary and base-isolated buildings are given in Fig. 5. These two models are almost identical except that different modeling techniques are used for the substructure connecting the basement slab and the first floor. More specifically, major

difference is in the middle portion of the support columns where the isolator is located. For the ordinary building, each basement column is represented by three beam elements in which the stiffness of the basement reinforced concrete wall is included. For the isolated building, on the other hand, the isolator is modeled by two spring elements; one linear spring and one nonlinear elastoplastic spring to simulate, respectively, the vertical and horizontal responses of the isolator. Two beam elements, similar to those columns of the superstructure are then utilized above the below the isolator to model the reinforced concrete pedestals.

To facilitate the numerical simulation, separate models are employed to analyze the horizontal responses in the transverse (X) and longitudinal (Y) directions. In these models only input accelerations at the basement nodes and building boundary conditions are different due to differences in the direction of seismic excitation. Other input data are identical.

In calculating the horizontal response of the isolator a bilinear force-displacement constitutive equation is used for the nonlinear spring element. This relationship is determined from the dynamic tests of ANL bearings conducted by the Shimizu Corporation [2]. The stiffness used in the SISEC code analysis is given in Fig. 6.

In addition to the stiffness, the damping ratio of the isolator is also an important parameter for the numerical simulation. As discussed in section II and also evident from Fig. 4b it is seen that the damping ratio obtained from the site experiment, corresponding to 0.4 cm (0.16 in) horizontal displacement, is about 10%. For this range the damping ratio obtained from the site experiment is lower if the relative displacement is smaller. Since the maximum isolator displacement obtained from the preliminary calculations is only 0.15 cm (0.06 in), an extrapolated damping ratio of 7.25% is thus used in the SISEC code simulations.

As a first step, the 3-D frame model of the ordinary building is used to study the fundamental building characteristics. Results of the SISEC model analysis revealed that the frequencies of the first two modes are 3.57 and 4.15 Hz. They correspond to the transverse (X) and longitudinal (Y) directional vibrations, respectively. The frequencies of the test building in these two directions obtained by the Shimizu Corporation of Japan are 3.63 and 4.38 Hz. The agreement of predicted and measured frequency characteristics is quite good.

IV.   RESULTS AND DISCUSSIONS

Data of three representative earthquakes, i.e., #2, #6, and #17 are used here to study the building response characteristics. However, because of space limitation, emphasis is placed on earthquake #6 which has the largest peak magnitude.

In simulating the responses of ordinary and isolated buildings, the X (transverse) and Y (longitudinal) component accelerations observed at the center of the basement of the isolated building are utilized as input to the basement structural nodes. The computed accelerations are then compared with those of observations.

A.   Earthquake #2

This earthquake occurred on April 28, 1989 less than twelve hours after all in-situ tests were completed. The earthquake had a magnitude of 4.9 and an epicentral distance of 102 km.

For simplicity, comparison of observed and calculated peak accelerations at the first floor and the roof level of both ordinary and isolated buildings are given in Table 1. As can be seen from this table, the maximum accelerations obtained from recorded data and SISEC simulations

8

agree satisfactorily with each other. However, at the roof level of the isolated building, the simulated accelerations are about 16% lower than those observed.

It is interesting to study the effects of the embedment of the ordinary building and the isolation system of the isolated building on the building responses. As mentioned before in Section II, the ordinary building has a 6.56 ft (2 m) embedment which would reduce the acceleration response during this small seismic event. This can be seen from the observed accelerations and their frequency values. For instance, in the transverse (X) direction, the observed peak accelerations at the basement and first floor are 7.55 and 9.25 gal [3.13 and 3.64 in/sec^2], respectively; and both of them have a dominant frequency of 2.57 Hz. This suggests that the first floor and basement of the ordinary building almost move as a rigid body during the seismic excitation. The embedment also has a restraining effect on the roof acceleration response. However, its effect is difficult to be quantatively assessed.

Because of the small earthquake motion and embedment of the ordinary building, the advantage of base isolation in mitigating the acceleration response is not visible. In fact, at the first floor, accelerations observed in both directions of the isolated building are higher than the corresponding values of the ordinary building. This is also true for the other two earthquakes, #6 and #17, to be presented later. At the roof level, we have found that the transverse acceleration of the isolated building is slightly lower than that of the ordinary building. However, in the longitudinal direction, the trend is reversed; the peak acceleration of the isolated building is larger.

B.   Earthquake #6

This earthquake occurred quite near the test building on June 24, 1989. It has a magnitude of 4.4 and epicentral distance of about 6 km from the test facility. The earthquake caused the largest ground accelerations at the ground surface when compared with other earthquakes detected between April and December, 1989.

Figure 7 provides observed accelerations in the transverse (X) and longitudinal (Y) directions at the basement of the isolated building. The maximum accelerations corresponding to these two directions are 34 and 19 gal [13.11 and 7.43 in/sec^2], respectively. These values are higher than those of other earthquakes. These recorded acceleration time histories were used in time-history analyses of building responses.

Since the isolation device is designed to protect the structure against strong earthquakes, the advantage of using base isolation system for earthquake #6 is thus more pronounced. We will proceed to describe the results of the comparison.

1.   Ordinary Building

The observed and calculated transverse (X-direction) accelerations of the first floor are given in Fig. 8. Excellent comparison has been found, not only for the peak values and the times of occurrence, but also the response shapes and characteristic frequencies. Figure 9 depicts the comparison of roof accelerations in the transverse (X) direction. As can be seen from these figures, both accelerations correlated very well with each other. However, the maximum accelerations differ by 28%. Such deviation may be attributed to the lack of soil-structure-interaction treatment of the embedment of ordinary building in the numerical simulation. Also,

it is noted from the analytical results that the roof vibrates with a frequency approximately 3.50 Hz, which value compares satisfactorily with the field test result of 3.63 Hz obtained by the Shimizu Corporation of Japan.

In the longitudinal (Y) direction, the recorded and simulated acceleration histories at the first floor are given in Fig. 10. Excellent comparison of the accelerations can be seen from this figure. The shape of the time histories, peak values, and frequency characteristics all closely resemble each other. Both observation and simulation indicate that the amplification of the first floor acceleration is small. Because of the relatively large ground acceleration, the first floor oscillates with a dominant frequency of 4.20 Hz which is quite different from that of the ground motion. This implies that the effect of the embedment on the response of the first floor is small.

At the roof level, the observed and calculated accelerations are presented in Fig. 11. Both figures show that major seismic events occur between 10 to 15 seconds and gradually damp out around t = 30 sec. Exceptionally good comparison is found for the dominant frequency at the roof level, which has a value of 4.30 Hz. This frequency value, obtained from the time-history analysis, coincides with that of the model analysis.

2.   Isolated Building

Input accelerations for simulating the transverse (X) and longitudinal (Y) responses of the isolated buildings have been presented previously in Fig. 7. The two components of ground acceleration have dominant frequencies of 2.53 and 2.23 Hz, respectively. Numerical simulations are carried out with a computer code through 3000 cycles of computation with a 0.01 sec constant integration step.

11

In the transverse direction, comparison of the recorded and simulated accelerations at the first floor is shown in Fig. 12. Good agreement again has been found from these acceleration responses. Peak accelerations especially compare well. The maximum recorded acceleration is about 39 gal (15.15 in/sec^2), almost duplicates with the simulated value of 40.45 gal (15.92 in/sec^2). Note that the floor response is dominated by a frequency of 2.07 Hz which agrees closely with the simulated frequency of 2.13 Hz. This frequency corresponds to the frequency of the isolator in responding to the seismic event. Also, analytical results indicate that the 3.40 Hz building frequency has been filtered out through the use of base isolation.

Figure 13 depicts the recorded and calculated acceleration histories at the roof of the isolated building. Reasonable correlation of the acceleration pulse is also obtained although the maximum acceleration is underpredicted by about 22%.

In the longitudinal direction, the observed and calculated accelerations at the first floor and roof are compared in Figs. 14 and 15. The trends of acceleration histories at the corresponding location, as well as the maximum accelerations, agree excellently. The deviations between the observed and simulated peak values are 19 and 8%, respectively, at the first floor and roof. At these two locations, the dominant frequency is found to be 2.23 Hz.

C.   Earthquake #17

This earthquake occurred at 03:26:15 on November 2, 1989. It features the longest excitation time, approximately 90 sec, compared to other earthquakes recorded between April and December, 1989. This long-duration seismic motion in conjunction with nonlinear behavior of isolator usually presents difficulties for the conventional finite-element programs. Since the SISEC code has salient capabilities of treating long-duration problems through a mixed-time

12

integration scheme and nonlinear isolator characteristics, it can be used to analyze such longer earthquakes without rendering into difficulties of excessive CPU time and numerical instabilities.

To facilitate the presentation, Table 3 lists the observed and simulated peak accelerations for both ordinary and isolated buildings. Again, due to the presence of soil embedment and a reinforced concrete wall in the basement of the ordinary building, no advantage of isolation system in reducing the acceleration response of the base-isolated building is seen. In fact, both observed and simulated results consistently indicate that for the isolated building the accelerations are greater than those of the unisolated building.

Results from Table 3 also reveal excellent correlation between analyses and observations. To illustrate the comparison, Fig. 16 provides observed and simulated longitudinal (Y-direction) accelerations on the roof level of the isolated building. Good agreement has been found, including the response shape, maximum, and minimum values, as well as times of occurrence.

V.   CONCLUSIONS

The data used for this benchmark test were obtained from the instrument measurements of full-size reinforced concrete structures located in Sendai, Japan. The data were derived from actual earthquakes. The data are of high quality and thus can be used with confidence for validation of the seismic system response program. These recorded data are also suitable for assessing the code calculational capabilities as well as the modeling techniques used in the analysis.

In the analytical simulation, two frame models were developed for calculating the seismic responses of the ordinary and base-isolated structures, respectively. The computer acceleration

responses are compared to those from observations. Also, the effect of base-isolation systems was investigated by comparing the dynamic characteristics of the base-isolated building with those of the ordinary building.

From the comparison of analytical solutions with actual recorded earthquake data, several conclusions can be drawn:

(1)   The numerical solution can reproduce the general shape of the acceleration responses, both for the ordinary and base-isolated buildings. The analysis accurately predicts the peak accelerations and the times of occurrence.

(2)   The analysis can accurately calculate the frequency characteristics of both ordinary and the isolated buildings. The computed frequencies of the ordinary building are about 3.50 and 4.20 Hz, respectively, in the transverse and longitudinal directions. The test building frequencies are about 3.60 and 4.35 Hz. For the isolated building, the simulated frequency is about 2.13 Hz, slightly lower than the 2.30 Hz obtained from the observation.

(3)   The SISEC code is very effective for simulating the seismic response of the base isolated structure. On the CRAY machine, the CPU time for calculating the 90-sec seismic event of earthquake #17 is 350 seconds. The equivalent CPU time for the IBM machine is about 30 minutes.

(4)   As anticipated, the advantage of isolation system for a small earthquake is insignificant. For relatively large earthquake motion, however, such as from records of #6 earthquake, the effect of isolators in reducing the roof-acceleration becomes more pronounced. For instance, for this earthquake, the computed amplification factor in the transverse direction of the isolated building is about 1.46, compared to 4.07 computed for the ordinary building.

14

(5)   The magnitude of earthquake #6 and corresponding horizontal displacements of the isolators are still considered to be small. It did not cause uplift and overturn to occur at the Sendai isolated building. Thus, the effects of uplift, overturning, and impacts of basemats cannot be assessed and compared from the current data base. Further validation of these effects is needed when strong earthquake data becomes available on much stronger ground motions.

ACKNOWLEDGMENTS

REFERENCES

1. R. I. Skinner, "Base Isolated Structures in New Zealand," Proc. Eighth WCEE, San Francisco, 1984, pp. 927-934.

2. A. G. Tanics, D. Way, and J. M. Kelley, "The Implementation of Base Isolation for the Foothill Communities Law and Justice Center," A report to the National Science Foundation and the County of San Bernadino, 1984, Reid and Tarics Associates, San Francisco, CA.

3. C. Plichon, R. Gueraud, M. H. Richli, and J. F. Casagrande, "Protection of Nuclear Power Plants Against Seism," Nuclear Technology, Vol. 49, pp. 295-306, 1980.

4. T. Kuroda, et al., unpublished information, 1989.

5. K. Tamura, H. Yamahara, and M. Izumi, "Proof Tests of the Base-Isolated Building Using Full-Sized Model," Proc. Seismic, Vibration, and Shock Isolation-1988, ASME, PVP-Vol. 147, pp. 21-28.

6. T. Kuroda, M. Saruta, and Y. Nitta, "Verification Studies on Base Isolation Systems by Full-Scale Buildings," Proc. Seismic, Vibration, and Shock Isolation-1989, ASME, PVP-Vol. 181, pp. 1-8.

7. R. F. Kulak and C. Y. Wang, "Design and Analysis of Seismically Isolated Structures," Post Conference Seminar of the 10th Intl. Conf. on Structural Mechanics in Reactor Technology (SMiRT-10), Proc. 1st Intl. Seminar on Seismic Base Isolation for Nuclear Power Facilities, CONF-8908221, pp. 341-368, San Francisco, CA, August 21-22, 1989.

Table 1. Comparison of Observed and Calculated Maximum
Accelerations for Earthquake #2

| Location | Direction | Maximum Acceleration, in/sec^2 | | | |
| | | Ordinary Building | | Isolated Building | |
		Obs.	Cal.	Obs.	Cal.
Roof	T(X)	10.82	10.61	8.83	6.68
	L(Y)	10.22	10.36	13.05	9.25
First Floor	T(X)	3.64	3.77	5.06	4.69
	L(Y)	3.65	5.72	6.57	6.64
Basement	T(X)			3.13	
	L(Y)			4.28	

T: Transverse
L: Longitudinal

Table 2. Comparison of Observed and Calculated Maximum
Accelerations for Earthquake #6

| Location | Direction | Maximum Acceleration, in/sec^2 | | | |
| | | Ordinary Building | | Isolated Building | |
		Obs.	Cal.	Obs.	Cal.
Roof	T(X)	41.85	53.48	24.71	19.26
	L(Y)	29.53	25.14	19.85	18.11
First Floor	T(X)	14.87	12.08	15.15	15.93
	L(Y)	8.28	9.02	12.97	15.46
Basement	T(X)			13.11	
	L(Y)		–	7.43	

T: Transverse
L: Longitudinal

17

Table 3. Comparison of Observed and Calculated Maximum
Accelerations for Earthquake #17

| Location | Direction | Maximum Acceleration, in/sec² | | | |
| | | Ordinary Building | | Isolated Building | |
		Obs.	Cal.	Obs.	Cal.
Roof	T(X)	16.25	18.92	22.74	19.08
	L(Y)	11.84	12.58	14.61	18.36
First Floor	T(X)	4.09	5.05	10.13	12.92
	L(Y)	5.06	5.41	9.54	14.64
Basement	T(X)			3.81	
	L(Y)			5.18	

T: Transverse
L: Longitudinal
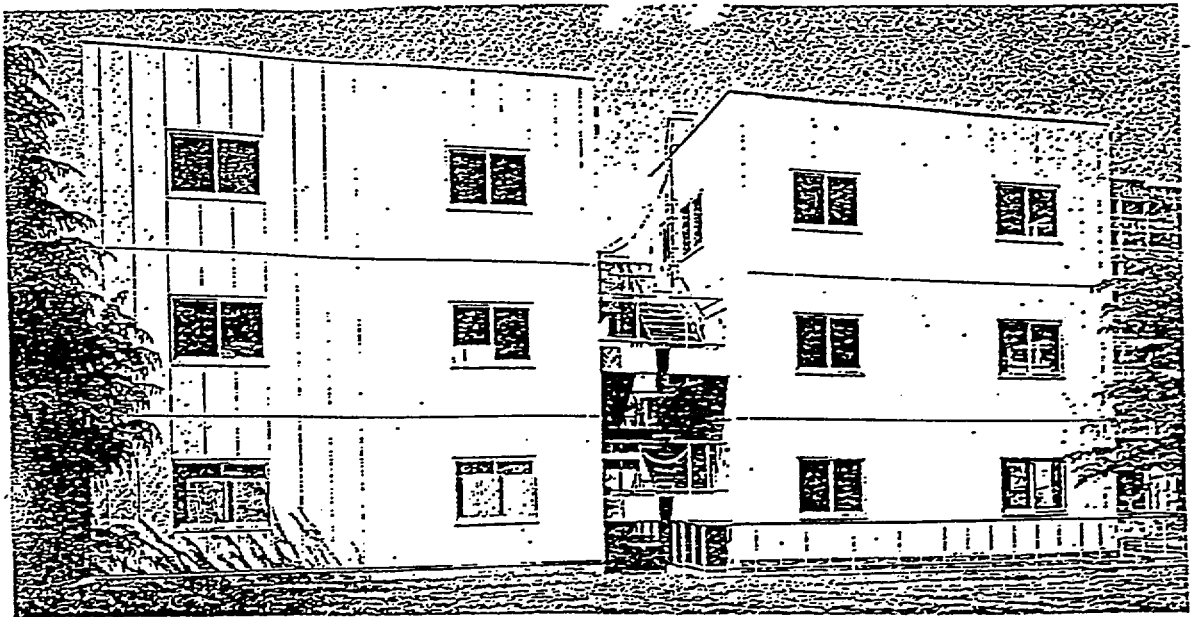
Fig. 1.   General View of Test Building
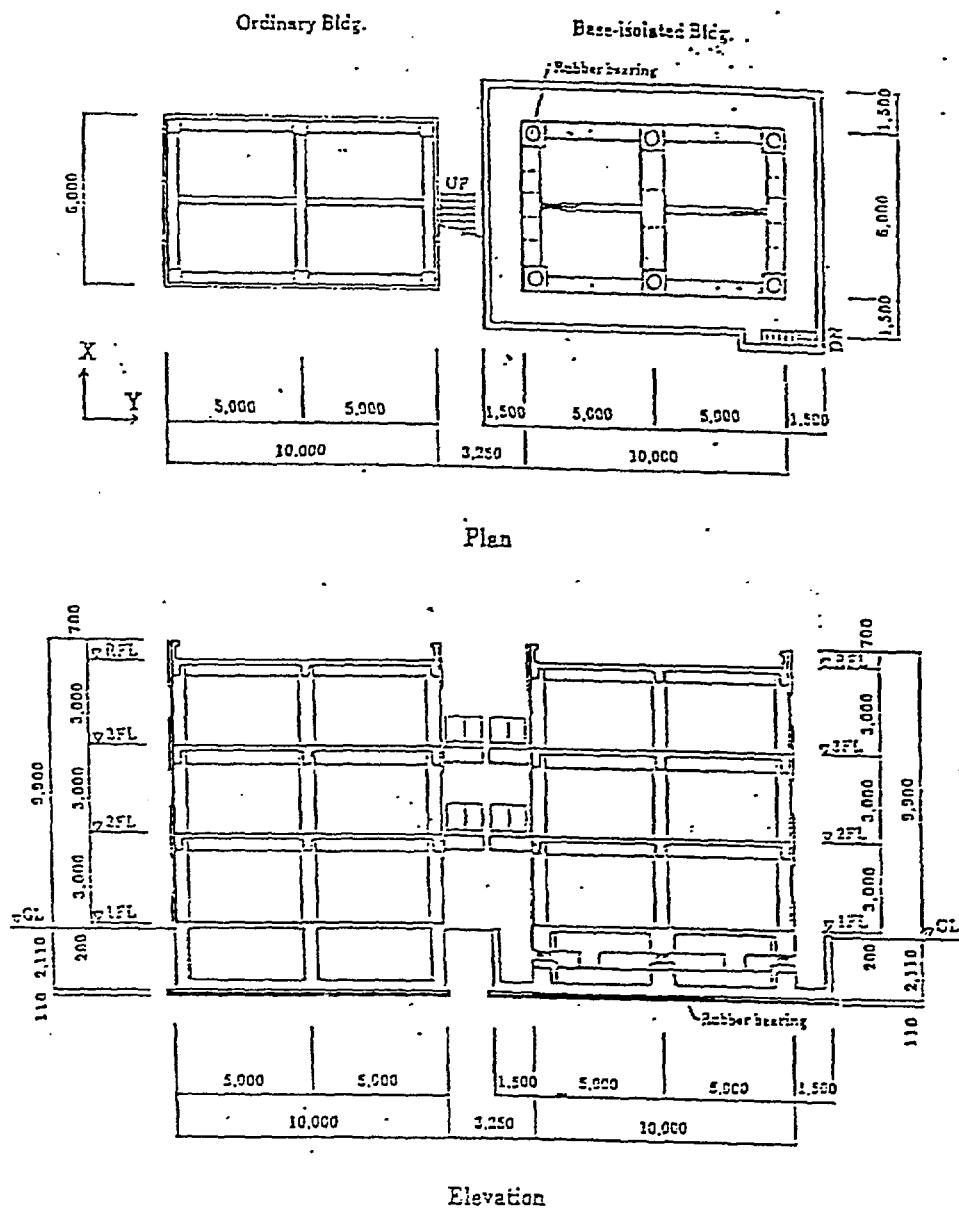
Fig. 2. Plan and Elevation Views of Test Building

15.9 11UNC-2A though
6.35 cover layer;
22.2 deep in plate

279.4

469.9

45°

45°

508.0

A'

A

Detail B

279.4

50.8

(A36)

6.35

25.4

204.2

RUBBER 4.85×33=160.1
(62 DURO NATURAL RUBBER)

SHIM   1.90 ×32=61.0
(A570 GR40)

220.9

25.4

6.35

19.1

469.9

508.0

19.1

Section A—A.

55.7

6.35

31.0

22.2

46.0

Detail B
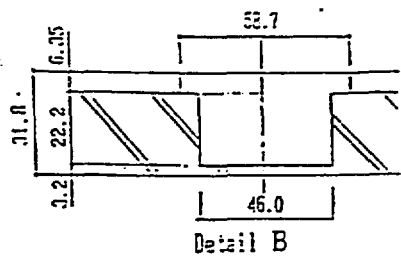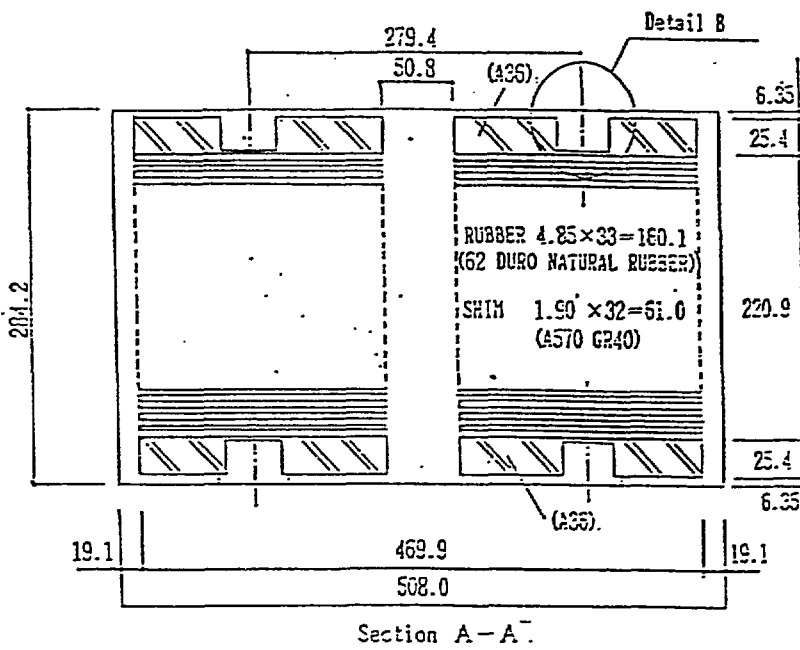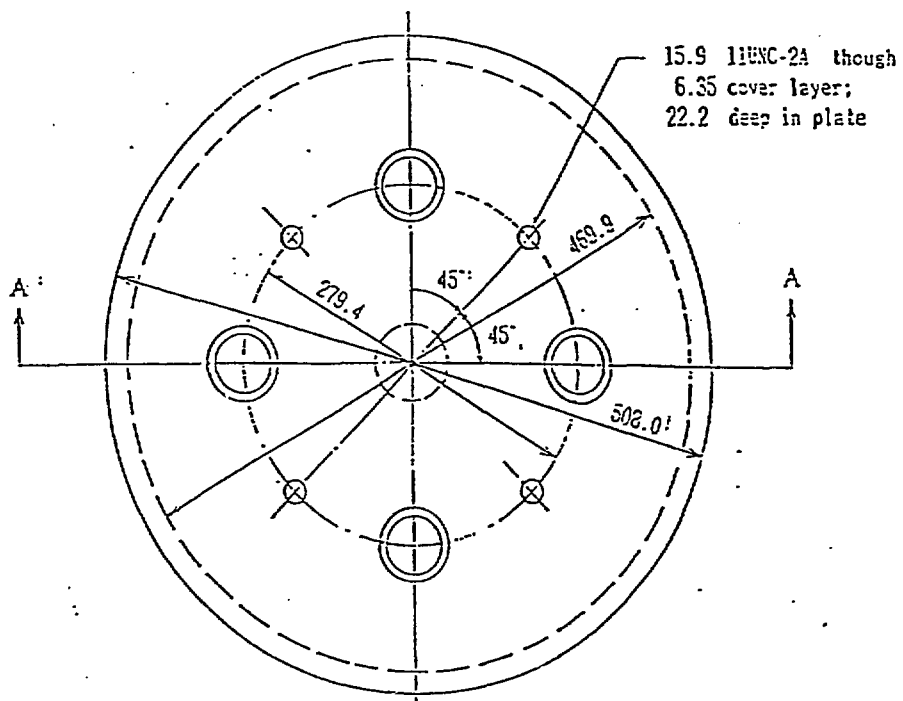
Fig. 3. Bearing Configuration and Dimensions (unit: mm)

(a) Equivalent Horizontal Stiffness

(b) Equivalent Damping Ratio
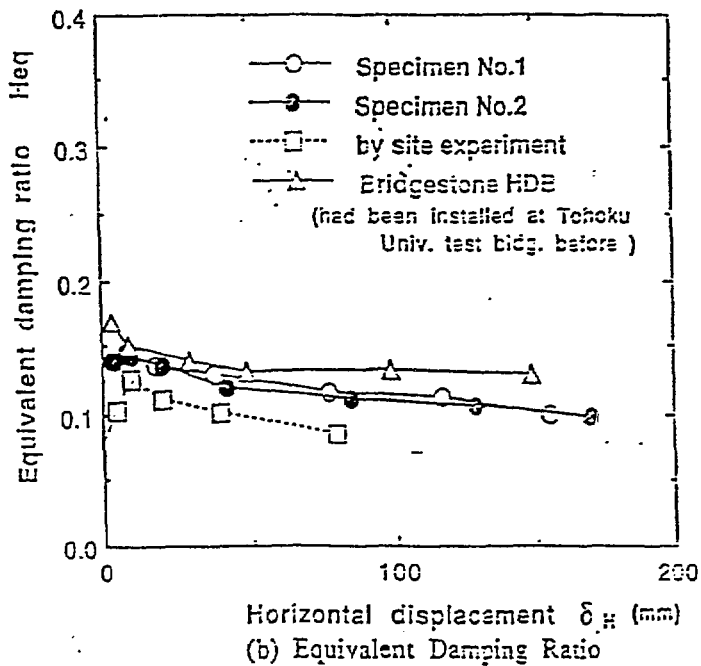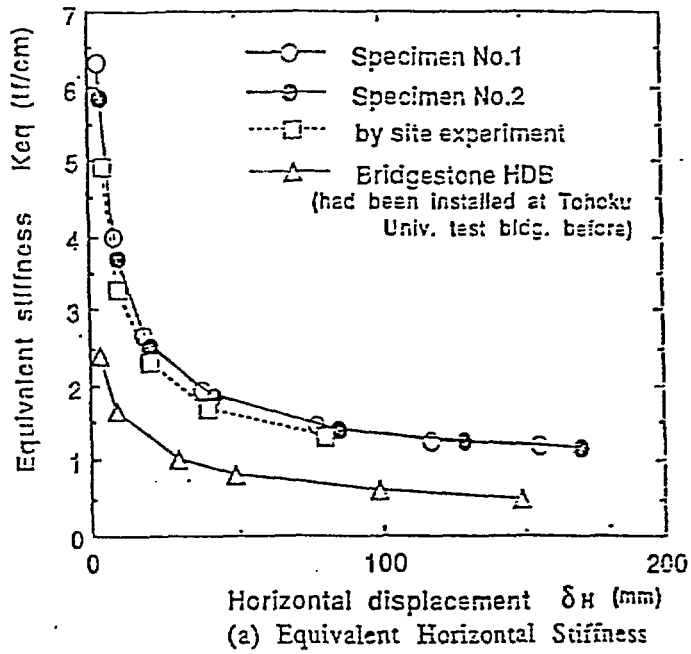
Fig. 4. Equivalent Horizontal Stiffness and Damping Ratio of Isolator

22

TIME = 0.000
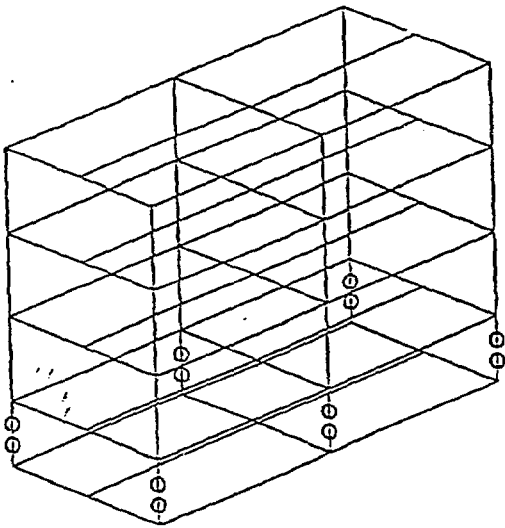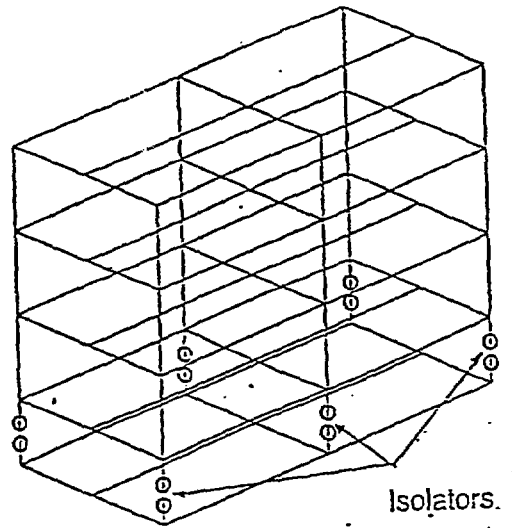
NO ISOLATION   WITH ISOLATION

Fig. 5. Mathematical Models of Ordinary and Isolated Buildings
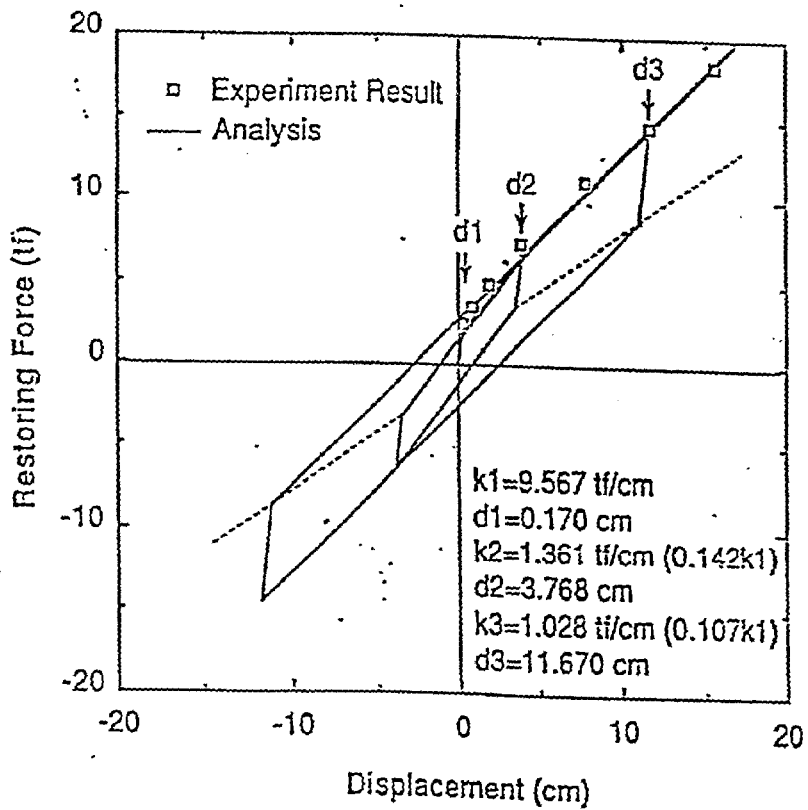
Fig. 6. Analytical Parameters for Simulating Isolator
Horizontal Response

The figure shows a graph of Restoring Force (tf) versus Displacement (cm) with:

- Legend: □ Experiment Result, — Analysis
- Labels d1, d2, d3 marking points on the curve

Parameters:
k1=9.567 tf/cm
d1=0.170 cm
k2=1.361 tf/cm (0.142k1)
d2=3.768 cm
k3=1.028 tf/cm (0.107k1)
d3=11.670 cm

ISOL. B. - OBS. ACCEL. FILE 06 - BASE (ANL22) TRANSVERSE

TMAX,AMAX TMIN,AMIN= 11.81   13.1181   12.02   -11.6529
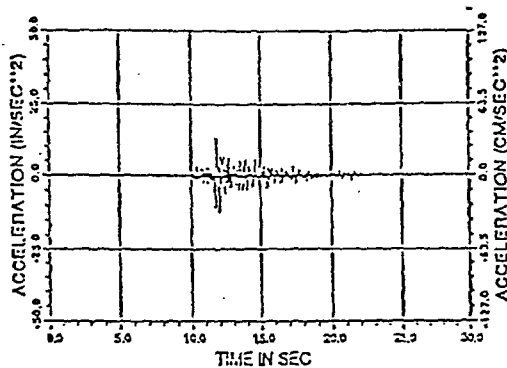
ISOL. B. - OBS. ACCEL. FILE 06 - BASE (ANL22) LONGITUD.

TMAX,AMAX TMIN,AMIN= 12.05   7.4031   11.57   -11.5512
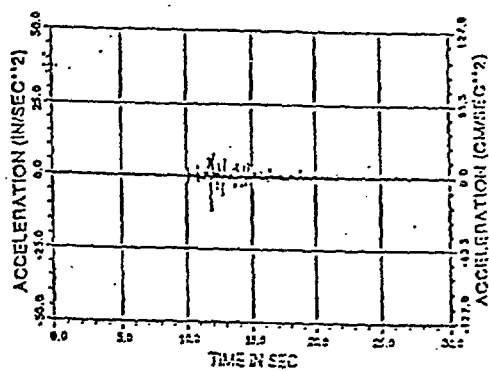
Fig. 7.   Acceleration histories used in the SISEC code simulations (left: transverse, right: longitudinal).

25

ORD. S. - OBS. ACCEL. FILE 05 - 1ST. FL. (ANL17) TRANSVERSE

TMAX,AMAX TMIN,AMIN= 11.51 14.8740 12.02 -15.5235

ORD. B. - CALC. ACCEL. FILE 05 - 1ST FL. (NODE 59) TRANSVERSE

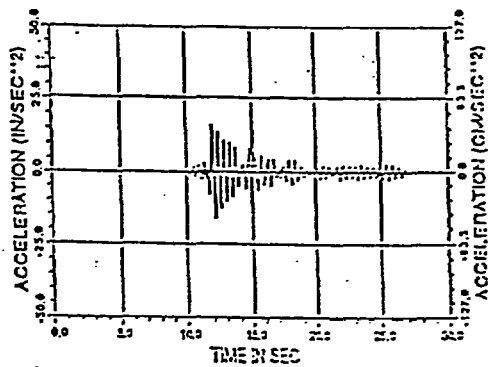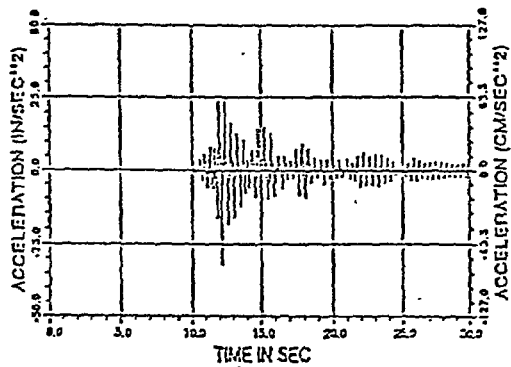TMAX,AMAX TMIN,AMIN= 11.93 1.2373'15' 12.04 -1.5572'16'
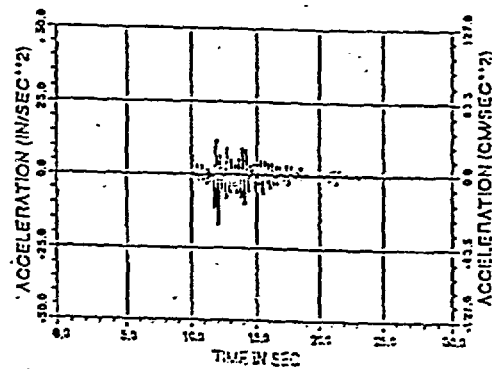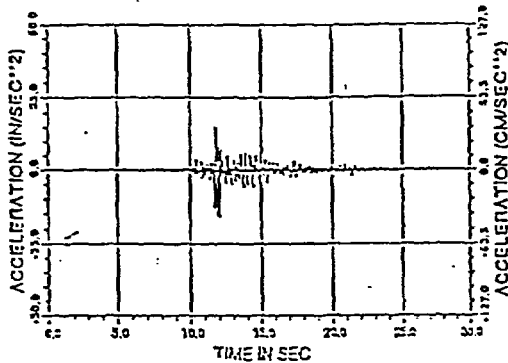
Fig. 8. Comparison of transverse accelerations at the first floor of the ordinary building (left: observed, right: calculated).

26

ORD. B. - OBS. ACCEL FILE 05 - ROOF (ANL20) TRANSVERSE

TMAX,AMAX,TMIN,AMIN= 12.18 41.8504 12.05 -40.2756
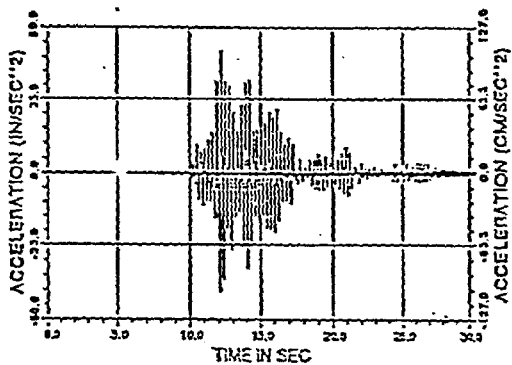
ORD. B. - CALC. ACCEL. FILE 05 - ROOF (NODE 5) TRANSVERSE

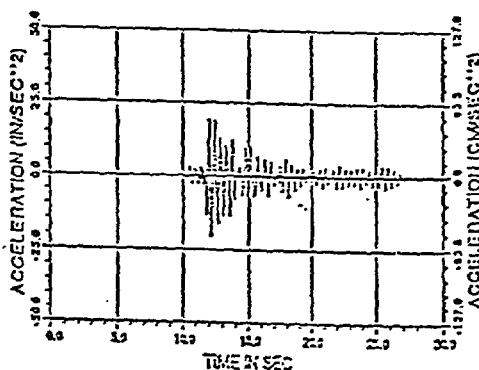TMAX,AMAX,TMIN,AMIN= 12.21 5.3457*10⁰ 12.04 -5.0852*10⁰
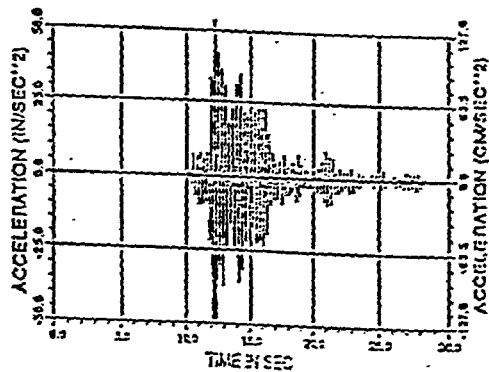
Fig. 9. Comparison of transverse accelerations at the roof of the ordinary building (left: observed, right: calculated).

ORD. B. - OBS. ACCEL FILE 05 - 1ST. FL. (ANL18) LONGITUD.

TMAX,AMAX TMIN,AMIN= 11.76 8.2755 11.87 -13.5102
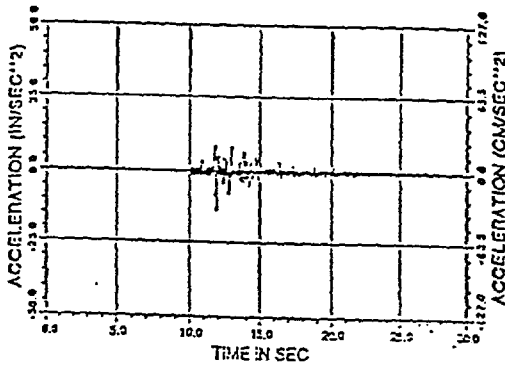
ORD. B. - CALC. ACCEL FILE 05 - 1ST FL (NODE 53) LONGITUD.
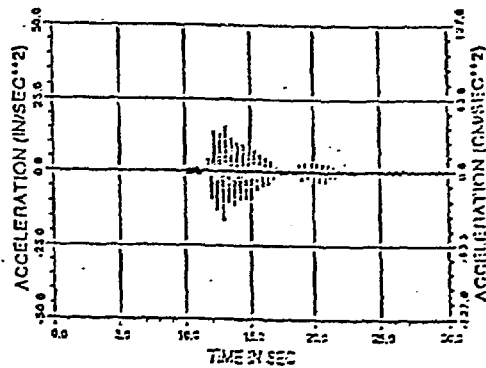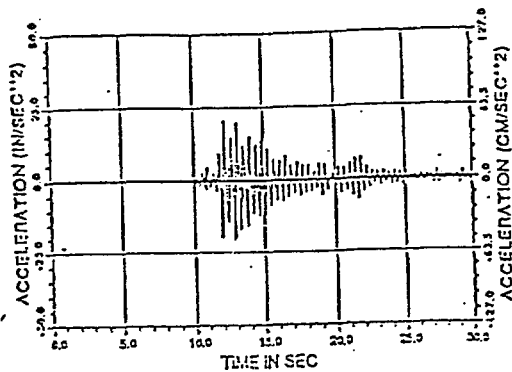
TMAX,AMAX TMIN,AMIN= 11.77 9.0192 11.89 -16.5557
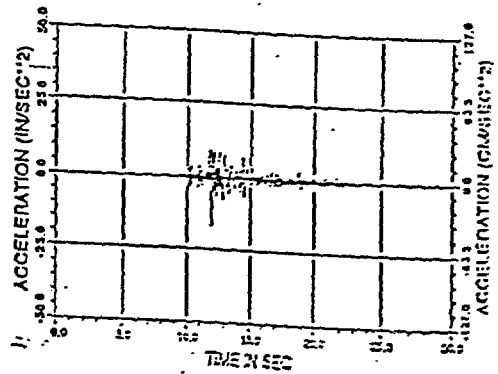
Fig. 10. Comparison of longitudinal accelerations at the first floor of the ordinary building (left: observed, right: calculated).

28

ORD. B. - OBS. ACCEL. FILE 05 - ROOF (ANL21) LONGITUD.

I.MAX.AMAX TMIN.AMIN= 14.08 29.5276 11.91 -20.0512

ORD. B. - CALC. ACCEL. FILE 06 - ROOF (NODE 5) LONGITUD.

TMAX.AMAX TMIN.AMIN= 12.58 25.1592 13.10 -22.6359
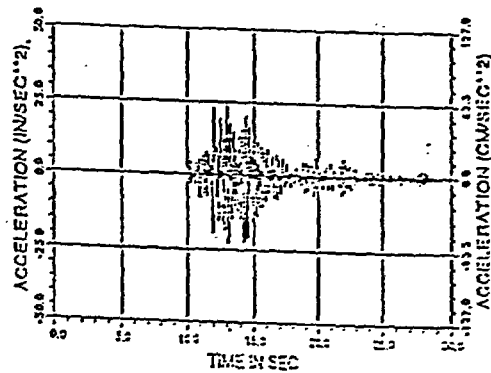
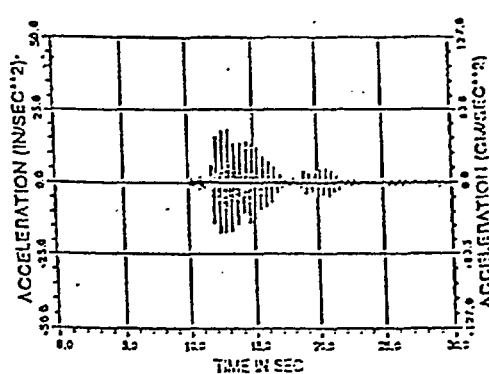Fig. 11. Comparison of longitudinal accelerations at the roof of the ordinary building (left: observed, right: calculated).

29

ISCL. B. - OBS. ACCEL. FILE C5 - 1ST. FL. (ANL26) TRANSVERSE   ISCL. B. - CALC. ACCEL. FILE C5 - 1ST FL. (NODE 55) TRANSVERSE

TMAX,AMAX TMIN,AMIN= 12.00 15.1457 12.23 -20.0569   TMAX,AMAX TMIN,AMIN= 11.57 15.5279 12.19 -15.5367
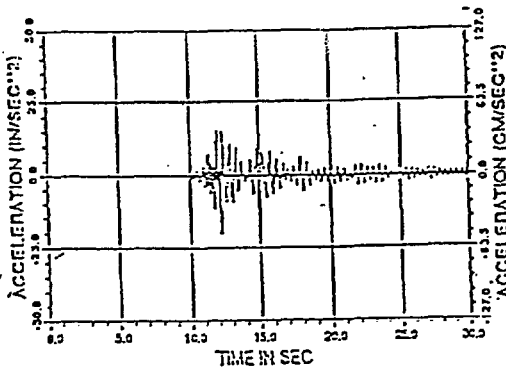
Fig. 12.   Comparison of transverse accelerations at the first floor of the
           isolated building (left: observed, right: calculated).

30
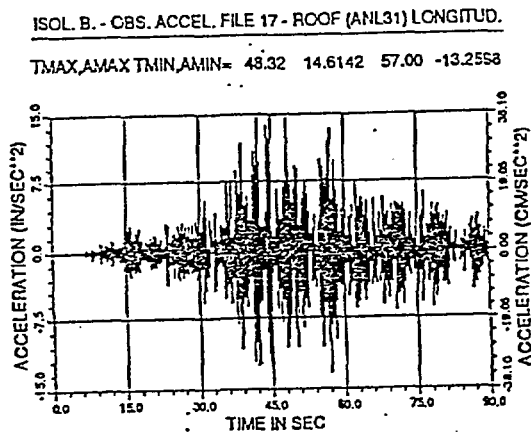
Fig. 13. Comparison of transverse accelerations at the roof of the isolated building (left: observed, right: calculated).

ISCL B. - OBS. ACCEL FILE 05 - 1ST. FL (ANL29) LONGITUD.

TMAX,AMAX TMIN,AMIN= 12.21 12.9565 12.41 -13.5760
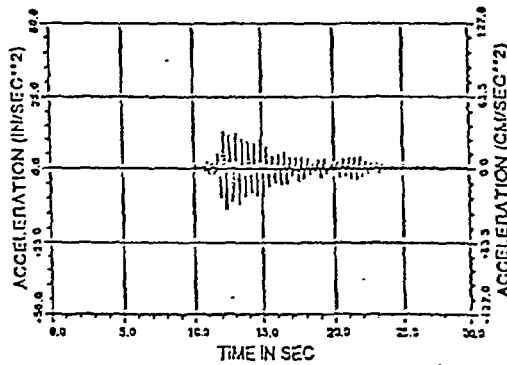
ISCL B. - CALC. ACCEL FILE 05 - 1ST FL (NODE 69) LONGITUD.

TMAX,AMAX TMIN,AMIN= 13.02 15.4565 12.66 -16.4291

Fig. 14. Comparison of longitudinal accelerations-at-the-first floor of
the isolated building (left: observed, right: calculated).

32

ISOL. B. - OBS. ACCEL. FILE 05 - ROOF (ANL31) LONGITUD.

TMAX,AMAX TMIN,AMIN= 12.16   19.8465   12.83 -20.1850

ISOL. B. - CALC. ACCEL. FILE 05 - ROOF (NODE 5) LONGITUD.

TMAX,AMAX TMIN,AMIN= 15.12   15.1651   12.44 -17.1504

Fig. 15.   Comparison of longitudinal accelerations at the roof of the isolated building (left: observed, right: calculated).

33

ISOL. B. - OBS. ACCEL. FILE 17 - ROOF (ANL31) LONGITUD.

TMAX,AMAX TMIN,AMIN= 48.32 14.6142 57.00 -13.2558

ISOL. B. - CALC. ACCEL. FILE 17 - ROOF (NODE 9) LONGITUD.

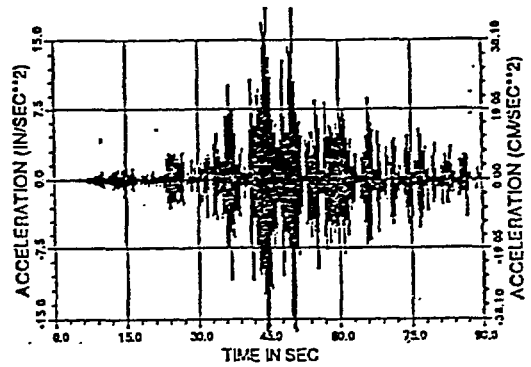TMAX,AMAX TMIN,AMIN= 45.10 18.2592 44.85 -16.4851

Fig. 16. Comparison of Longitudinal Acceleration at the Roof of the Isolated Building (left: observed, right: calculated)

34